

## Unusual Phase Diagrams of a Two-Component Coulomb Fermi Liquid

G. Kirczenow and K. S. Singwi

*Department of Physics and Astronomy and Materials Research Center,  
Northwestern University, Evanston, Illinois 60201*

(Received 9 January 1979)

Microscopic calculations of the phase diagrams of a two-component degenerate Coulomb Fermi liquid—the electron-hole liquid in ⟨111⟩-stressed Ge—have been made for various values of stress. The coexistence curves for three-phase equilibrium which summarize the most interesting features of these phase diagrams are reported. A particularly striking case which occurs at lower stress is one in which the two liquid phases coexist in two separate temperature ranges.

In recent years, the phase diagram of a mixture of the quantum liquids He<sup>3</sup> and He<sup>4</sup> has been studied.<sup>1</sup> The coexistence of two fluid phases consisting of nuclei and a sea of nucleons in neutron stars has also been explored theoretically.<sup>2</sup> However, little or nothing is known concerning the phase diagrams of a mixture of two Coulomb Fermi liquids although this constitutes the simplest two-fluid quantum system and should be amenable to a detailed microscopic study. Experimentally such a system is realizable in the electron-hole liquid (EHL) in a Ge crystal homogeneously stressed along the ⟨111⟩ direction.

In this Letter we report on the most interesting aspect of the phase diagrams of this system, i.e., the coexistence curves for three-phase equilibrium. Our calculations reveal that this system exhibits a rich variety of phase diagrams. The ⟨111⟩ stress raises three of the Ge conduction

valleys while lowering the fourth. In pure samples “hot” electrons in the EHL can be trapped in the three higher valleys for a time  $\sim 1$   $\mu$ sec before decaying into the lower (“cold”) valley.<sup>3</sup> This is a sufficiently long time for the hot electrons to thermalize within the three higher valleys, although their Fermi level remains different from that of the cold electrons in the lower valley. If one ignores the slow transfer of electrons between different valleys, the hot and cold electrons behave thermodynamically as two different species in quasiequilibrium with each other and with the holes. We shall show that under suitable conditions the above system separates into two distinct liquids each made up of hot (*h*) and cold (*c*) electrons and holes (*H*) but different in composition in so far as the ratio of *h* to *c* is concerned. The liquid phases are in equilibrium with a vapor containing all three species.

The free energy  $F$  of the EHL can be written as

$$F(N_h, N_c, N_H, V, T) = F_h^0(N_h, V, T) + F_c^0(N_c, V, T) + F_H^0(N_H, V, T) + F_{xc}(N_h, N_c, N_H, V, T), \quad (1)$$

where  $N_h$ ,  $N_c$ ,  $N_H$ , and  $V$  are the numbers of hot electrons, cold electrons, holes, and the volume, respectively.  $F_h^0$ ,  $F_c^0$ , and  $F_H^0$  are the free energies of *noninteracting* gases of hot electrons, cold electrons, and holes, respectively. Since  $N_h + N_c = N_H$ , only two of the component species can be varied independently. When only one electron species is present, good results have been obtained by approximating  $F_{xc}$  at metallic *densities*, by its  $T=0$  value  $E_{xc}$ .<sup>4,5</sup> We also use this approximation. We make the further simplification that the exchange-correlation energy density  $E_{xc}/V$  depends only on the total density of the hot and cold electrons in the EHL and not on the way in which the electrons are distributed among the different conduction valleys. This approximation is valid as explained recently.<sup>6</sup>

To compute the phase diagram of the EHL, we need the pair chemical potentials  $\mu_h$ ,  $\mu_c$ , and the

pressure  $p$ . With the above approximations on  $F$ , these are

$$\begin{aligned} \mu_h &= \mu_h^0 + \mu_H^0 + \mu_{xc}, \\ \mu_c &= \mu_c^0 + \mu_H^0 + \mu_{xc}, \\ p &= p_h^0 + p_c^0 + p_H^0 + p_{xc}, \end{aligned} \quad (2)$$

where  $\mu_i^0 = (\partial F_i^0 / \partial N_i)_{V, T}$ ,  $p_i^0 = -(\partial F_i^0 / \partial V)_{N_i, T}$ ,  $\mu_{xc} = (\partial E_{xc} / \partial N)_{V, T}$ , and  $p_{xc} = -(\partial E_{xc} / \partial V)_{N, T}$ . Here  $i$  can be *h*, *c*, or  $H = N_h + N_c$ . The  $\mu_i^0$  and  $p_i^0$  are given by

$$p_i^0 = \int_0^\infty dE \nu_i(E) / \{ \exp[\beta(E - \mu_i^0)] + 1 \}$$

and

$$n_i = \beta \int_0^\infty dE \frac{\nu_i(E) \exp[\beta(E - \mu_i^0)]}{\{ \exp[\beta(E - \mu_i^0)] + 1 \}^2},$$

where  $d\nu_i(E)/dE$  is the density of states and  $n_i$

$=N_i/V$ . For the nonparabolic valence band,  $\nu_i(E) = E^{3/2}f(E/S_H)$ , where  $S_H$  is the valence-band splitting at  $\vec{k}=0$  and  $f$  is calculated numerically<sup>7</sup> using the results of Pikus and Bir<sup>8</sup> and of Hensel and Suzuki.<sup>9</sup> For the electrons,  $f$  is a constant. This guarantees that in the limit  $N_h \rightarrow 0$ ,  $N_c$  finite, we recover for  $\mu_h$  the correct logarithmic asymptotic behavior of dilute solutions.<sup>10</sup> For a given  $n_i$  we calculate  $\mu_i^0$  and then  $p_i^0$ . Because  $E_{xc}$  is not sensitive to the details of band structure, we use for it numerical values which correspond to a model band structure which is simpler than that of the stressed Ge. We have used a model band structure corresponding to unstressed Ge and the numerical values of  $E_{xc}$  denoted "Model I, SPH" by Bhattacharyya *et al.*<sup>11</sup> This choice of  $E_{xc}$  results in Ge EHL ground-state densities which are in very good agreement with experiment at zero stress and at all values of  $\langle 111 \rangle$  uniaxial stress for which data are available.<sup>7</sup>

Since in almost all experiments the EHD occupies only a small volume in the crystal, the liquid is always in contact with vapor. We shall focus our attention on the restricted but particularly interesting region of the phase diagram where all three phases coexist. This region is described according to the Gibbs phase rule,

$$f = C - P + 2$$

(here  $C=2$ ,  $P=3$  and therefore  $f=1$ ), by plotting the coexistence curves. At this stage of development of the experimental art we believe this to be the most pertinent information.

The condition for phase equilibrium is that the pressure and each of the two chemical potentials be the same in all phases. This requires the simultaneous solution of six equations for three-phase equilibrium. At  $T=0$  the vapor phase can be ignored and  $p=0$ . The results for this case were reported earlier.<sup>6</sup> For  $T \neq 0$ , two temperature regimes require different treatments for the vapor phase.

(i) At low temperatures ( $T \lesssim 3^\circ\text{K}$ ) the gas consists of excitons whose vapor pressure is very low. We set  $p=0$  and solve the equations

$$\mu_h^{\text{II}} = \mu_h^{\text{I}}, \quad \mu_c^{\text{II}} = \mu_c^{\text{I}}, \quad (3)$$

for the two liquid phases I and II. We find that the  $p=0$  approximation is very good.

(ii) At high temperatures, the vapor phase is metallic so that Eq. (2) is used to calculate both the liquid and gas phases. An estimate of the density above which the vapor is metallic can be ob-

tained by setting the Debye-Hückel screening length equal to the exciton Bohr radius. This corresponds to a density  $n \lesssim 10^{15}/\text{cm}^3$ , which is much smaller than the vapor density in the temperature region in which we use this approach. Our method of solving the equations consists in evaluating  $n$ ,  $\mu_h$ , and  $\mu_c$  as functions of the concentration  $x = n_h/n_c$  for fixed  $T$  and  $p$ . We then examine different values of  $p$  and find the one for which  $\mu_h$  and  $\mu_c$  are the same in the three phases.

The results for some typical stress values are shown in Figs. 1–3. It should be borne in mind that these figures represent the coexistence curves for three phases in equilibrium. At a given temperature each of the three coexisting phases is characterized by its own concentration  $x$  and density  $n$  shown in the upper and lower part of each figure. At lower temperatures we only plot  $x$  and  $n$  for the two liquid phases I and II. At higher temperatures the curve for the vapor is

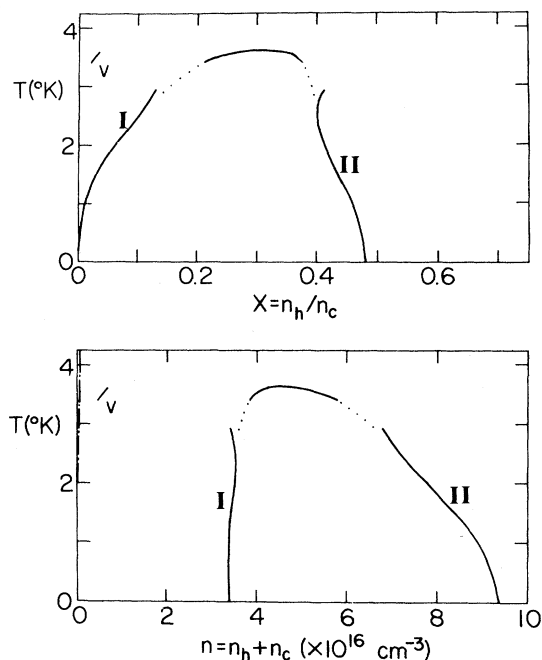


FIG. 1. Coexistence curves for three phases in equilibrium for a valence-band splitting  $S_H$  of 4 meV. The values of the concentration  $x$  and total density  $n$  for each phase are plotted for various temperatures. The liquid phases are labeled I (with a smaller concentration of hot electrons) and II (with a larger concentration of hot electrons).  $v$  denotes the coexisting vapor phase. Dotted lines, smooth interpolation between the high- and low- $T$  regions; dot-dashed curve, density at which the Debye-Hückel screening length equals the exciton Bohr radius (177 Å).

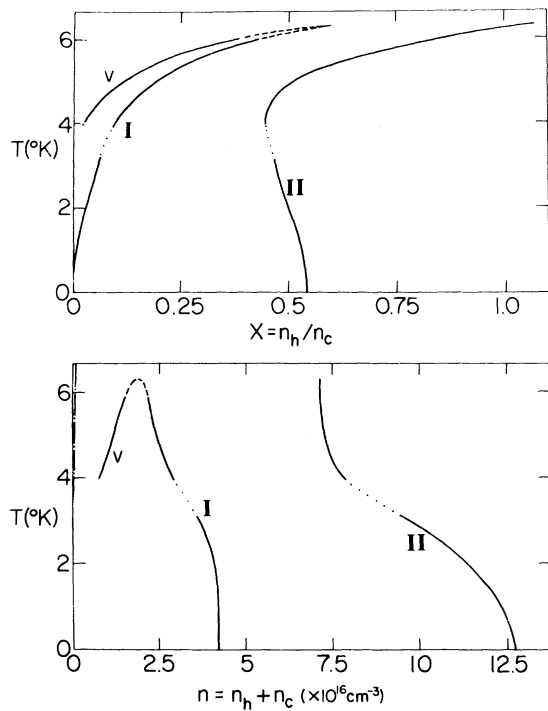


FIG. 2. Coexistence curves for three phases in equilibrium for a valence-band splitting  $S_H$  of 3 meV. Notation is as in Fig. 1. For explanation of dashed curves, see text.

labeled  $v$ .

The coexistence curves contain the information necessary to delineate the region of the phase diagram (in  $\bar{n}_h - \bar{n}_c - T$  space) in which the three phases coexist. It is easy to show that for a given  $T$  this region has a triangular cross section in  $\bar{n}_h - \bar{n}_c$  space. The bar denotes the average density of the species and the vertices of the triangle have the coordinates  $(n_h, n_c)$ ,  $n_h$  and  $n_c$  being the actual densities in the respective phases. A detailed discussion of the phase diagrams will be given elsewhere.

At low temperatures the system contains two liquid phases which behave *differently* as the temperature rises for different values of stress. At  $S_H = 4$  meV (Fig. 1) the two liquid phases dissolve in each other at a critical temperature of solution between 3 and 4°K. The vapor curve  $v$  ends abruptly at this critical temperature since we are interested only in three-phase equilibria. In the temperature region in which the curves are shown dotted we do not calculate the coexistence curves because the density in the vapor phase is such that neither approximation (i) nor (ii) is valid. In the lower-temperature region, we use

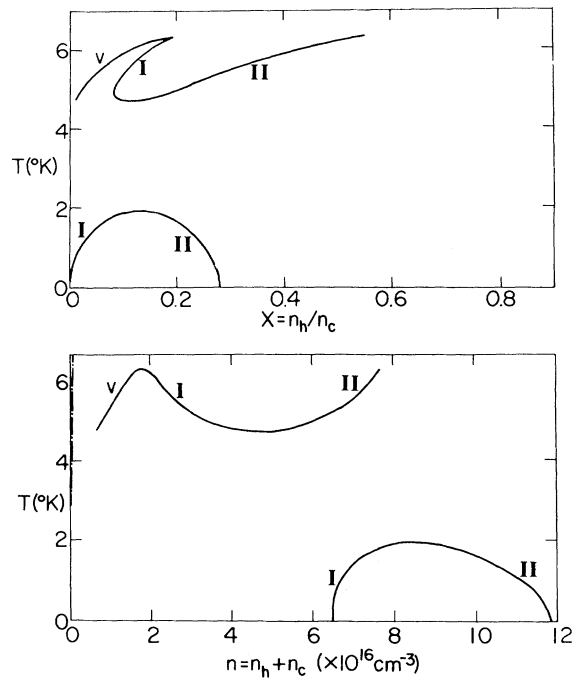


FIG. 3. Coexistence curves for three phases in equilibrium for a valence-band splitting  $S_H$  of 1.5 meV. Notation is as in Fig. 1.

approximation (i).

At a stress  $S_H = 3$  meV (Fig. 2) as the temperature increases the liquid phase II continues to exist as a separate phase while the less-dense liquid phase I and vapor merge. As is the case at zero stress, the liquid-vapor critical point (6–7°K) is quite sensitive to the numerical interpolation procedure<sup>12</sup> of  $E_{xc}$  and for this reason we have denoted part of the curve by broken lines. Notice that the form of the coexistence curves in Fig. 2 is very different from that in Fig. 1, which implies the same for the phase diagrams.

At a stress  $S_H = 1.5$  meV (Fig. 3) the behavior of the coexistence curves is particularly interesting. The system has two coexisting liquid phases at low temperatures, which dissolve into each other at  $T \sim 2^\circ\text{K}$ . For  $T \gtrsim 5^\circ\text{K}$  the system again exists as two liquid phases in equilibrium with vapor. When the temperature rises further the liquid phase I merges with the vapor. In the temperature range approximately 2–5°K it is not possible to have the two liquid phases simultaneously present. We find that this latter conclusion is valid irrespective of what pressure one assigns to the vapor phase. This remarkable behavior can be physically understood as follows. At very low temperatures the chemical potential  $\mu_h$  as a

function of  $x$  has a minimum which is responsible for the phase separation.<sup>6</sup> As the temperature increases, this minimum becomes shallower as a result of contributions to  $\mu_h$  from the temperature-dependent term ( $\sim -T^2/n_h^{2/3}$ ) which is a rapidly increasing function of  $x$ , and eventually the liquid phases coalesce. With further increase of temperature the EHL density begins to decrease rapidly. When the density has fallen to a point where the hole Fermi level is close to the valence-band separation, the system begins to make the maximum use of the nonparabolicity<sup>6</sup> of the valence band, thus offsetting the contribution from the temperature-dependent part of  $\mu_h$ . This again leads to a minimum in  $\mu_h$  as a function of  $x$  and the phase separation of the EHL reappears. It should be noted that the reappearance of the phase separation at higher temperatures is found also if the Hubbard values of  $E_{xc}$  are used; however, in this case the effect persists to somewhat higher values of stress.

In conclusion, we have shown explicitly from a microscopic calculation that the EHL in  $\langle 111 \rangle$ -stressed Ge exhibits a remarkable diversity of coexistence curves as function of stress which in turn implies a similar diversity of phase diagrams. The interesting phenomena which we have discussed occur in the temperature and stress ranges which are easily accessible to experiment and should, therefore, provide a stimulus for experimental work on a unique system. In practice the concentration  $x$  can be controlled in a time-resolved experiment.<sup>13</sup> One possible way to identify the phase separation would be to study the luminescence line shapes as a function of time.

We thank J. Bajaj, L. Liu, and G. Wong for helpful discussions. This work was supported in part under the National Science Foundation-Materials Research Laboratories program through the Ma-

terial Research Center of Northwestern University (Grant No. DMR 76-80847) and in part by the National Science Foundation Grant No. DMR 77-09937.

<sup>1</sup>See, for example, C. Ebner and D. O. Edwards, Phys. Rep. 2C, 78 (1971); J. M. Kincaid and E. G. D. Cohen, Phys. Rep. 22C, 58 (1975).

<sup>2</sup>G. Baym and C. Pethick, Annu. Rev. Nucl. Sci. 25, 27 (1975); J. M. Lattimer and D. G. Ravenhall, Astrophys. J., 223, 314 (1978).

<sup>3</sup>H.-h. Chou, G. K. Wong, and B. J. Feldmann, Phys. Rev. Lett. 39, 959 (1977).

<sup>4</sup>M. Combescot, Phys. Rev. Lett. 32, 15 (1974).

<sup>5</sup>The validity of the approximation is discussed by T. M. Rice, in *Proceedings of the Twelfth International Conference on the Physics of Semiconductors*, edited by M. H. Pilkuhn (B. G. Teubner, Stuttgart, 1974), p. 23.

<sup>6</sup>G. Kirzenow and K. S. Singwi, Phys. Rev. Lett. 41, 326, 1140(E) (1978).

<sup>7</sup>G. Kirzenow and K. S. Singwi, Phys. Rev. B 19, 2117 (1979). A model calculation of the EHL ground state in stressed Ge by A. A. Kastalskii, Fiz. Tverd. Tela 20, 1241 (1978) [Sov. Phys. Solid State 20, 715 (1978)] has just been brought to our notice. This calculation neglects valence-band structure and is in the Hartree-Fock approximation.

<sup>8</sup>G. E. Pikus and G. L. Bir, Fiz. Tverd. Tela 1, 1828 (1959) [Sov. Phys. Solid State 1, 136 (1959)].

<sup>9</sup>J. C. Hensel and K. Suzuki, Phys. Rev. B 9, 4219 (1974).

<sup>10</sup>L. D. Landau and E. M. Lifshitz, *Statistical Physics* (Pergamon, New York, 1969), p. 277.

<sup>11</sup>P. Bhattacharyya, V. Massida, K. S. Singwi, and P. Vashishta, Phys. Rev. B 10, 5127 (1974).

<sup>12</sup>T. M. Rice, in *Solid State Physics*, edited by H. Ehrenreich, F. Seitz, and D. Turnbull (Academic, New York, 1978), Vol. 32.

<sup>13</sup>H.-h. Chou, J. Bajaj, and G. K. Wong, J. Lumin. 18-19, 131 (1979).